about CH_5^+ from its high-resolution spectra and accompanying rotational structure. Indeed, this is where subtle but revealing effects of the end-over-end tumbling, nuclear spin statistics, and tunneling splittings will be addressed that can not be accurately treated in the present vibrational framework (29, 30). The detailed interpretation of the high-resolution spectrum of CH_5^+ and its isotopomers will clearly provide interesting opportunities for further theoretical and experimental challenges in this elusively fluxional species. Extensions of the present work to include deuterated analogs of CH_5^+ (31) and to probe the effects of rotations are currently under way.

References and Notes

1. O. Asvany et al., Science 309, 1219 (2005).
2. V. L. Tal'roze, A. K. Lyubimova, Dokladi na Bulgarskata Akademiya na Naukite SSSR 86, 909 (1952).
3. K. Hiraoka, K. P. Kebarle, J. Am. Chem. Soc. 97, 4179 (1975).
4. K. Hiraoka, T. Mori, Chem. Phys. Lett. 161, 111 (1989).
5. R. J. Saykally, Science 239, 157 (1988).
6. D. W. Boo, Z. F. Liu, A. G. Suits, J. S. Tse, Y. T. Lee, Science 269, 57 (1995).
7. E. T. White, J. Tang, T. Oka, Science 284, 135 (1999).
8. C. Savage, F. Dong, D. J. Nesbitt, paper presented at 60th International Symposium on Molecular Spectroscopy, Columbus, OH, 20–24 June 2005.
9. A. Olah, G. Rasul, Acc. Chem. Res. 30, 245 (1997).
10. A. Komornicki, D. A. Dixon, J. Chem. Phys. 86, 5625 (1987).
11. P. V. Schleyer, J. W. D. Carneiro, J. Comput. Chem. 13, 997 (1992).
12. P. R. Schreiner, S. J. Kim, H. F. Schaefer, P. V. Schleyer, J. Chem. Phys. 99, 3716 (1993).
13. H. Müller, W. Kutzelnigg, J. Noga, W. Klopper, J. Chem. Phys. 106, 1863 (1997).
14. For a review through 2000, see (32).
15. A. Brown, B. J. Braams, K. Christoffel, Z. Jin, J. M. Bowman, J. Chem. Phys. 119, 8790 (2003).
16. A. B. McCoy et al., J. Phys. Chem. A 108, 4991 (2004).
17. A. Brown, A. B. McCoy, B. J. Braams, Z. Jin, J. M. Bowman, J. Chem. Phys. 121, 4105 (2004).
18. K. C. Thompson, D. L. Crittenden, M. J. T. Jordan, J. Am. Chem. Soc. 127, 4954 (2005).
19. Z. Jin, B. Braams, J. M. Bowman, J. Phys. Chem. A, Hase Festschrift Issue, in press; appeared online as an ASAP article, 5 October 2005 doi: 10.1021/jp053848o.
20. D. Marx, M. Parrinello, Nature 375, 216 (1995).
21. D. Marx, M. Parrinello, Science 271, 179 (1996).
22. D. Marx, M. Parrinello, Z. Phys. D 41, 253 (1997).
23. J. Tse, D. D. Klug, K. Laasonen, Phys. Rev. Lett. 74, 876 (1995).
24. The quantum DMC method used in this work has been described previously [see (16, 17)]. Specifically, the simulations were run for 5025, time steps of 10 atomic time units, with α = 0.1 H. The probability amplitudes were obtained using the descendent weighting approach, counting the number of descendents of each walker after 25 time steps. To obtain the weightings used to average the spectra obtained at each of the stationary points, we calculated the probability amplitude near each of the three stationary points and averaged the results from 16 evaluations of the probability amplitudes. This yielded relative probabilities of 38% at the C_s(I) minimum, 41% at the C_{2v} saddle point, and 22% at the C_s(II) saddle point.
25. J. M. Bowman, S. Carter, X. Huang, Int. Rev. Phys. Chem. 22, 533 (2003).
26. N. I. Hammer et al., J. Chem. Phys. 122, 244301 (2005).
27. The MULTIMODE calculations were performed in rectilinear normal modes. By including a large degree of mode-mode coupling and vibrational configuration interaction procedures, curvilinear motions are accurately described by this approach. The present calculations of the spectrum were done using a four-mode representation of the potential and CI matrices on the order of 5000 for each symmetry block (A' and A" for C_s calculations and A_1, A_2, B_1, and B_2 for the C_{2v} calculation). A 5MR calculation was done at the C_{2v} reference geometry, with CI matrices on the order of 15,000 for each symmetry block. The zero-point energy obtained with this large calculation is 10,989 cm^{-1}, which is close to the exact quantum DMC result of 10,908 ± 5 cm^{-1}. The 5MR energies for fundamental excitations of importance in the calculated spectrum are roughly 20 to 30 cm^{-1} lower than those from the 4MR calculations used to obtain the spectrum.
28. A more complete description of the slit discharge apparatus with application to high-resolution jet-cooled spectra of molecular ions can be found in (33).
29. M. P. Deskevich, D. J. Nesbitt, J. Chem. Phys. 123, 084304 (2005).
30. P. R. Bunker, B. Ostojic, S. Yurchenko, J. Mol. Struct. 695-696, 253 (2004).
31. X. Huang, L. M. Johnson, J. M. Bowman, A. B. McCoy, in preparation.
32. P. R. Schreiner, Angew. Chem. Int. Ed. Engl. 39, 3239 (2000).
33. F. Dong, D. Uy, S. Davis, M. Child, D. J. Nesbitt, J. Chem. Phys. 122, 224301 (2005).
34. We thank the authors of (1) for sharing experimental data, as well as D. Marx for illuminating correspondence about their classical spectral calculations. This work was supported by grants from the National Science Foundation (J.M.B., A.B.M., D.J.N.), the Office of Naval Research (J.M.B.), and the Air Force Office of Scientific Research (D.J.N.). C.S. acknowledges support from a National Research Council postdoctoral fellowship.

Planktonic Foraminifera of the California Current Reflect 20th-Century Warming

David B. Field,[1]*† Timothy R. Baumgartner,[2] Christopher D. Charles,[1] Vicente Ferreira-Bartrina,[2] Mark D. Ohman[1]

It is currently unclear whether observed pelagic ecosystem responses to ocean warming, such as a mid-1970s change in the eastern North Pacific, depart from typical ocean variability. We report variations in planktonic foraminifera from varved sediments off southern California spanning the past 1400 years. Increasing abundances of tropical/subtropical species throughout the 20th century reflect a warming trend superimposed on decadal-scale fluctuations. Decreasing abundances of temperate/subpolar species in the late 20th century indicate a deep, penetrative warming not observed in previous centuries. These results imply that 20th-century warming, apparently anthropogenic, has already affected lower trophic levels of the California Current.

Records of various marine populations reveal that large declines in some marine algae, zooplankton, fish, and seabirds in the California Current in the late 20th century were linked to widespread ecosystem changes throughout the North Pacific in the mid-1970s (1–8). The associated change in environmental conditions resembled a sustained El Niño–like state, whereby greater cyclonic activity of the atmospheric Aleutian Low Pressure System was accompanied by warming in the eastern North Pacific (1–14). The origin of this ecosystem "regime shift" (15, 16) has been a source of debate since its detection. On one hand, changes in marine populations are often attributed to decadal-scale fluctuations in ocean-atmosphere conditions that are characterized by the Pacific Decadal Oscillation (PDO) (1). On the other hand, the ecosystem shift could reflect penetration of a greenhouse gas–induced warming in the global ocean (17–19) that exceeded a threshold of natural variability. A major difficulty with attribution of cause is the short length of most time series of climate and ecosystem variability. The debate is further complicated by the fact that variations in many marine populations could result directly from other anthropogenic influences (such as habitat disturbance or fishing) and/or indirectly by trophic cascades. It is therefore difficult to distinguish threshold effects of a warming trend on marine populations from decadal-scale variability or other anthropogenic influences.

We present paleoceanographic evidence to show that populations of planktonic foraminifera in the California Current were strongly affected by a 20th-century warming trend. Planktonic foraminifera have been used extensively in paleoceanographic studies. They function at a low trophic level and their species-specific sensitivities to preferred hydrographic conditions link their temporal variations to changes in

[1]Scripps Institution of Oceanography, University of California, San Diego, La Jolla, CA 92093, USA. [2]Centro de Investigación Científica y de Educación Superior de Ensenada, Km 107 Carretera Tijuana-Ensenada, Ensenada, Baja California, C.P. 22860, Mexico.

*Present address: Monterey Bay Aquarium Research Institute, 7700 Sandholdt Road, Moss Landing, CA 95039, USA.
†To whom correspondence should be addressed. E-mail: dfield@mbari.org

climate and primary productivity, with little evidence for controls of these assemblages by higher trophic levels (20–29). Our analysis builds on previous studies of variations in foraminiferal abundances in Santa Barbara Basin (SBB) sediments across El Niño and stadial/interstadial events (20–22) as well as studies of species-specific preferred habitats near the SBB (22–28). Although the SBB lies within an upwelling environment, regional- and basin-scale processes are considered more influential than high-frequency, local processes (3, 4, 12–14). The major interannual, decadal, and secular variations observed in sea surface temperature (SST) and zooplankton abundance at or near the SBB clearly follow the same patterns of variability observed coherently throughout the California Current (3, 4, 12–14, 30). Thus, foraminifera preserved in SBB sediments provide a rare opportunity to compare 20th-century marine ecosystem conditions with those from previous centuries.

A continuous high-resolution record from SBB sediments results from high sedimentation rates and the regular occurrence of anoxic bottom waters, which inhibit bioturbation. Thus, seasonal alternations in the deposition of lithogenic and biogenic particles result in well-defined annual laminae that can be counted visually to develop a reliable chronology (31).

A principal components analysis (PCA) of the temporal variations in foraminiferal abundance from SBB sediments collected with a Soutar box corer in 2001 captures two main patterns of variability in the most abundant species over nearly 300 years (Fig. 1). The first principal component (PC1) involves a substantial 20th-century increase in the abundance of species of primarily tropical and subtropical affinities, along with a decrease in the abundance of *Neogloboquadrina pachyderma* (sin.), a species with subpolar to polar affinity. The second pattern (PC2) involves species with

known temperate to polar affinities. The amplitudes of these two PCs covary on multiannual to decadal time scales ($P < 0.001$) until about 1959, when they begin to diverge (32). Postdepositional dissolution of tests cannot explain these patterns because species with both high and low resistance to dissolution have opposite loadings on the PCs (Fig. 2). Furthermore, comparing the amplitudes of the PCs with the averaged abundance of the same species constituting these PCs from separate SBB box cores taken in different years shows that the main temporal patterns are found in all cores and are detectable by different analytical approaches (Fig. 3) (32).

The temporal variability of PC1 reflects the principal multiannual to secular changes in SST over the past century (Fig. 3). This connection is not surprising because many of the tropical and subtropical species have symbiotic algae and favor environments with different combinations of higher SSTs, deeper thermoclines, and accompanying higher light levels (22–27). Therefore, anomalous near-surface warming and stratification, particularly in summer and fall, would expand the duration and extent of these species' preferred habitats and, consequently, their fluxes to the sediment (22–27). The association of *Globigerina bulloides* with PC1 is unexpected because it is typically associated with upwelling and/or conditions of high productivity. However, for *G. bulloides*, a threshold of unfavorable productivity can be reached during strong springtime upwelling in the nearby San Pedro Basin (23). In the SBB, the greatest fluxes of *G. bulloides* occur in spring of an anomalously warm year (e.g., 1997) and, more typically, in summer (22, 25). Thus, the
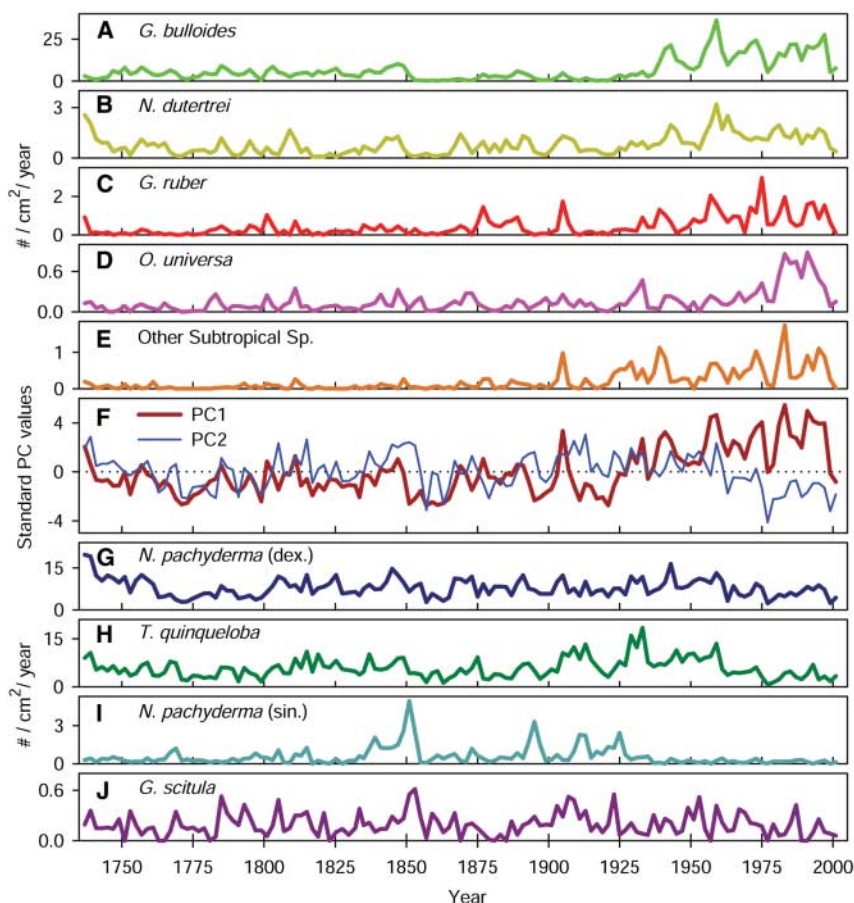

Fig. 1. Fluxes of planktonic foraminifera in Santa Barbara Basin (SBB) sediments from box core BC3001. (**A** to **E**) Taxa illustrating a significant trend ($P < 0.0001$ for each species) toward increasing abundances in the 20th century: (A) *G. bulloides*, (B) *N. dutertrei*, (C) *Globigerinoides ruber*, (D) *O. universa*, and (E) other subtropical species. (**G** to **J**) Species showing no temporal trend: (G) *N. pachyderma* (dex.), (H) *T. quinqueloba*, (I) *N. pachyderma* (sin.), and (J) *Globorotalia scitula*. (**F**) Temporal amplitudes of the first two principal components of the log-normalized time series of these species' abundances. PC1 and PC2 explain 40% and 21% of the total variance, respectively. Species loadings on PC1 and PC2 are shown in Fig. 2. "Other subtropical species" comprises the combined abundances of *Globigerinella calida*, *Globoturborotalita rubescens*, *Globigerinita glutinata*, *Globigerinella siphonifera*, and *Globigerinella digitata*, each of which occurred too infrequently to include individuality.
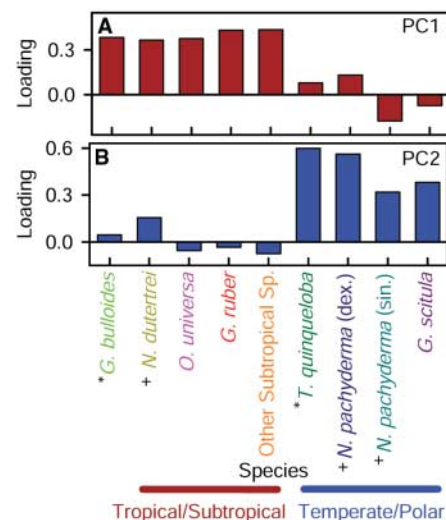

Fig. 2. Species loadings on PC1 and PC2, together with biogeographic affinities and dissolution susceptibility. Note that both species with high resistance to dissolution (+) and species with greater susceptibility to dissolution (*) have a range of opposing loadings on the two PCs.

association of *G. bulloides* with PC1 apparently reflects a preference for enhanced near-surface stratification during conditions of shoaling of isotherms (perhaps because prey would be more concentrated under these conditions than with a strictly isothermal water column). Accordingly, we interpret PC1 as the foraminiferal response to anomalous near-surface temperatures that modify stratification across the annual cycle of shoaling and deepening of isotherms.

The abundances of the deeper dwelling species that constitute PC2 generally increase with shallower isotherms and a cooler water column in this region of the California Current (*22–28*). However, there is also evidence that a strongly isothermal water column and very high productivity can be unfavorable for several of these species (*22–24*). Thus, their optimal environmental conditions would include some stratification, but less than for *G. bulloides* or other species associated with PC1. Accordingly, we interpret the time series of PC2 as primarily reflecting subsurface thermal adjustments to local and basin-wide wind fields and heat flux.

The covariation of PC1 and PC2 for much of the past few hundred years preceding the late 20th century indicates that some near-surface warming in the eastern Pacific can result in favorable environmental conditions for most species. Fluxes of species associated with PC1 would increase during late summer and fall, whereas species associated with PC2 (and *G. bulloides*) would generally increase during winter, spring, and summertime upwelling events. In addition, there may also be an increase in upwelling favorable winds during warm periods, because this has been observed during stadial events (*20*) and the late–20th-century warming (*12, 13, 33*). Nonetheless, upper ocean heat content has strongly increased in the late 20th century because the effect of atmospheric warming overwhelms the potential cooling effect of wind-induced shoaling of

isotherms (*12–14*). Fluxes of species associated with PC2 decreased in the late 20th century as the deep, penetrative warming passed a threshold of optimum stratification, unlike prior warming events.

The obvious increases in abundance of several taxa through the 20th century (Fig. 1) can be placed into better perspective by comparing equivalent size fractions of *G. bulloides*, *Orbulina universa*, and *Neogloboquadrina dutertrei* from the box core records with those from a longer Kasten core record over the past 1400 or 1000 years (Fig. 4). The elevated abundance of *G. bulloides* in the 20th century is unique in comparison with any prior point over the past 1000 years. The sustained high abundance of *O. universa* after the mid-1970s is also particularly unusual. The 20th-century increases in *N. dutertrei* are moderate, relative to both previous centuries and the previous 1400 years. The unprecedented abundance maxima in two of three species examined shows that the foraminiferal fluxes in the late 20th century are not simply an extreme form of common decadal-scale variability.

The combination of persistently higher fluxes of tropical/subtropical species and higher maximum fluxes in the 20th century indicates that background climatic conditions may serve to amplify the effect of El Niño variability, and to diminish the effect of La Niña variability, on marine populations in the California Current. Although there is no evidence for a permanent shift in the duration, magnitude, or frequency of the El Niño–Southern Oscillation in the past several centuries (*34*), the greatest peaks in abundance of most species associated with PC1 coincide with the largest and most extended El Niño events observed in the California Current with instrumental records (Figs. 1 and 3). Also, the strong La Niña event of 1999 marks one of the coolest periods observed in many instrumental records within the past 55 years (*6*). However, unlike cool periods of previous centuries, the subpolar species *N. pachyderma* (sin.) did not increase in abundance; this species has been nearly absent for 70 years.

Visual inspection of PC1 indicates that the secular trend began around 1925, a time that matches the rise in regional and global SSTs (Fig. 3) (*35*). In models, ocean warming occurs in the early 20th century in response to the accumulation of greenhouse gases, but relatively deep mixing in most regions diffuses the warming throughout the water column to a magnitude that is less than background variability (*19*). The increase in PC2 along with PC1 indicates that increasing SSTs in the early 20th century were accompanied by relatively shallow isotherms, which would result in a stronger thermal gradient. A more stratified water column would inhibit deep mixing and concentrate the early expression of any greenhouse gas–induced warming in the near-surface, which in turn might explain the strong involvement of
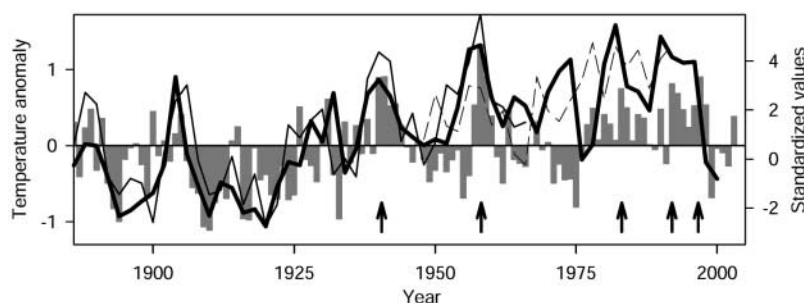

Fig. 3. Comparison of PC1 (bold solid line) with the SST record from the updated Kaplan reconstruction for the 5° × 5° grid centered at 122.5°W, 32.5°N (vertical bars) in the California Current near the SBB. PC1 is correlated with variations in SST from comparable 2-year averages of SSTs ($r^2 = 0.33$; $P < 0.001$). Arrows indicate strong El Niño events in the California Current. Also shown is the agreement of foraminiferal variations from PC1 (core BC3001) with those from two other cores in the SBB. Thin dashed line illustrates variations in averaged abundance of the same species loaded on PC1 from a core taken in 1992 and analyzed in this study. Thin solid line illustrates average of the principal species loaded on PC1 (*G. bulloides*, *N. dutertrei*, *G. ruber*, *O. universa*, and the combination of *G. calida* and *G. siphonifera*) from a core taken in 1969 and analyzed by A. Soutar and W. Berger.

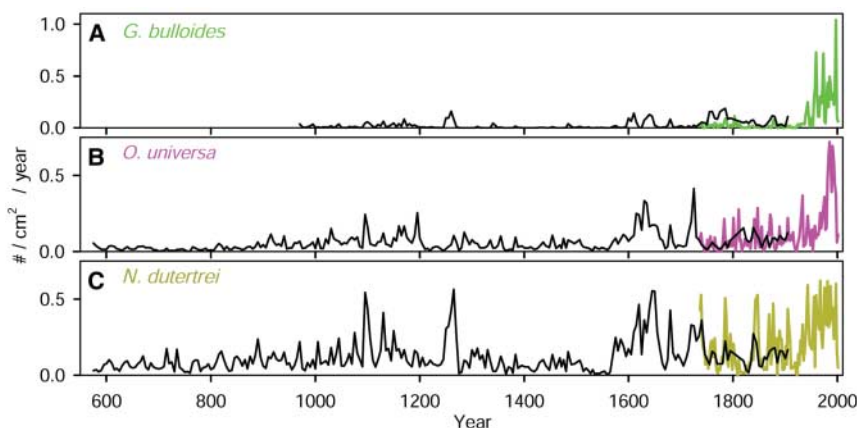**Fig. 4.** Comparison of abundances of (**A**) *G. bulloides*, (**B**) *O. universa*, and (**C**) *N. dutertrei* in the 300- to 500-µm size fraction from 5-year sampling intervals in Kasten core sediments with abundances of the same species and size fractions from 2-year sampling intervals of box core sediments. The record in (A) is shorter because this species was not enumerated from the earliest strata.

the California Current region with the average warming trend in the global ocean (*35, 36*). Our findings point to the possibility that anthropogenic warming has affected marine populations since the early 20th century, although only the ocean warming of the late 20th century has been confidently attributed to the accumulation of greenhouse gases (*17–19*).

Probably the most distinctive change in the foraminiferal record is the divergence in the time series of PC2 from the trend in PC1 that begins around 1960 and denotes a deeper penetration of the near-surface warming. This divergence reaches a maximum after the mid-1970s, coinciding with the well-documented change in climate and ecosystem throughout the North Pacific (*1–14*). The changes in foraminifera parallel decreases in the abundance of many taxa of algae, zooplankton, fish, and seabirds associated with temperate environments together with increases in many other tropical and subtropical taxa in the California Current (*1–7*). A recent study indicates that nonlinear biological responses to linear fluctuations in the physical environment play an important role in the ecosystem "regime shift" of the mid-1970s (*16*). Although it might be true that the foraminiferal response to SST and hydrography is also nonlinear (e.g., the response to different combinations of SST and thermocline structure), the divergence of the PCs in recent decades indicates that the trend in ocean heat content can also play an important role in the variations of some pelagic organisms.

The long-term warming trend described here helps to clarify how the mid-1970s regime shift in the North Pacific may be associated with atmospherically driven warming. It is well known that ocean changes since the mid-1970s are linked to an intensification of the atmospheric Aleutian Low Pressure System, which was partially driven by tropical SSTs (*9–11*). Atmospheric indices and tree ring–based reconstructions of the PDO indicate that the intensified Aleutian Low since the mid-1970s is the most persistent on record (*1, 9, 37, 38*). More important, coral records indicate that the elevated tropical SSTs that drive cyclonic activity exceed prior decadal variability and were likely forced by greenhouse gases (*11, 34, 39*). Thus, although variations in the Aleutian Low are a component of natural variability, the late 20th century experienced unusual tropical forcing as well as increased atmosphere-driven heat flux to the ocean.

Foraminifera provide one of the clearest examples of a direct influence of an ocean warming trend on marine ecosystems because (i) their variability is more clearly related to hydrographic conditions than to trophic cascades resulting from anthropogenic activities occurring in the 20th century, (ii) a consistent time series of observations can be extended back hundreds of years, and (iii) the California Current region is strongly related to the average

warming trend in the global ocean (*35*). Our results indicate that the variability of foraminifera in the California Current in the 20th century is linked to variations in SST and is atypical of the preceding millennium. Given that the trend in global SSTs has been attributed to increases in greenhouse gases in the atmosphere (*17–19*), it follows that the best explanation for this ecosystem aberration is anthropogenic warming that has passed a threshold of natural variability. As the warming of the ocean and atmosphere is likely to continue into the foreseeable future, the atypical state of the ocean over the period of most scientific observations must also be borne in mind for effective monitoring and management of living marine resources.

References and Notes

1. N. J. Mantua, S. R. Hare, Y. Zhang, J. M. Wallace, R. C. Francis, *Bull. Am. Meteorol. Soc.* **78**, 1069 (1997).
2. C. C. Ebbesmeyer *et al.*, *Calif. Dept. Water Res. Interagency Ecol. Stud. Prog. Rep.* **26**, 129 (1991).
3. D. Roemmich, J. McGowan, *Science* **267**, 1324 (1995).
4. J. A. McGowan, D. R. Cayan, L. M. Dorman, *Science* **281**, 210 (1998).
5. E. Brinton, A. Townsend, *Deep-Sea Res. II* **50**, 2449 (2003).
6. B. E. Lavaniegos, M. D. Ohman, *Deep-Sea Res. II* **50**, 2473 (2003).
7. M. J. Tegner, P. K. Dayton, P. B. Edwards, K. L. Riser, *CalCOFI Rep.* **37**, 111 (1996).
8. D. M. Karl, R. R. Bidigare, R. M. Letelier, *Deep-Sea Res. II* **48**, 1449 (2001).
9. K. E. Trenberth, J. W. Hurrell, *Clim. Dyn.* **9**, 303 (1994).
10. A. J. Miller, D. R. Cayan, T. P. Barnett, N. E. Graham, J. M. Oberhuber, *Oceanography* **7**, 21 (1994).
11. N. E. Graham, *Science* **267**, 666 (1995).
12. F. B. Schwing, R. Mendelssohn, *J. Geophys. Res.* **102**, 3421 (1997).
13. E. Di Lorenzo, A. J. Miller, N. Schneider, J. C. McWilliams, *J. Phys. Oceanogr.* **35**, 336 (2005).
14. D. M. Palacios, S. J. Bograd, R. Mendelssohn, F. B. Schwing, *J. Geophys. Res.* **109**, C10016 (2004).
15. J. D. Isaacs, *CalCOFI Rep.* **18**, 34 (1976).
16. C. Hsieh, S. M. Glaser, A. J. Lucas, G. Sugihara, *Nature* **435**, 336 (2005).
17. T. P. Barnett *et al.*, *Science* **309**, 284 (2005); published online 2 June 2005 (10.1126/science.1112418).
18. S. Levitus *et al.*, *Science* **292**, 267 (2001).
19. T. P. Barnett, D. W. Pierce, R. Schnur, *Science* **292**, 270 (2001).
20. I. L. Hendy, T. F. Pedersen, J. P. Kennett, R. Tada, *Paleoceanography* **19**, PA3007 (2004).
21. C. B. Lange *et al.*, *Mar. Geol.* **78**, 153 (1987).
22. D. E. Black, R. C. Thunell, E. J. Tappa, *Geology* **29**, 1075 (2001).
23. L. R. Sautter, R. C. Thunell, *J. Foraminifer. Res.* **21**, 347 (1991).
24. D. B. Field, thesis, Scripps Institution of Oceanography, University of California, San Diego (2004).
25. E. Kincaid *et al.*, *Deep-Sea Res. II* **47**, 1157 (2000).
26. J. D. Ortiz, A. C. Mix, R. W. Collier, *Paleoceanography* **10**, 987 (1995).
27. D. B. Field, *Paleoceanography* **19**, PA2014 (2004).
28. In an analysis of plankton samples taken in the California Current (*27*), 64%, 59%, and 35% of the variance in abundance of three of the four principal species that load positively on PC2 [*Turborotalia quinqueloba*, *N. pachyderma* (dex.), and *N. pachyderma* (sin.), respectively] is explained by the depth of the 11.5°C isotherm or another isopleth (*24*). An additional 12% of the variance in abundance of *T. quinqueloba* is explained by SSTs (greater abundance with lower SST). Also, it is well

known that *N. pachyderma* (sin.) is more abundant with lower SSTs in this region of the California Current (*20*).
29. C. Hemleben, M. Spindler, O. R. Anderson, Eds., *Modern Planktonic Foraminifera* (Springer-Verlag, New York, 1989).
30. There is a strong relationship between annual averages of monthly temperature anomalies at 10 m depth from the SBB with the annual Kaplan SST index (e.g., Fig. 3) for the 5° × 5° grid centered at 122.5°W, 32.5°N ($r^2 = 0.53$, $P < 0.0001$) and with annual anomalies of Scripps Pier SST ($r^2 = 0.54$, $P < 0.0001$). SBB anomalies are from measurements of station 82.47 (over the SBB) from the California Cooperative Oceanic Fisheries Investigations from 1950 to 2000. The analysis includes only years in which three or more measurements were available and no year had more than nine measurements (mode = 4). For comparison, the relationship between annually averaged monthly anomalies of more continuous time series of Scripps pier SST and the Kaplan SST index ($r^2 = 0.61$) is slightly higher. These large-scale patterns of coherent SST variability are consistent with analyses in (*3, 4, 13, 14*).
31. See supporting material on *Science* Online.
32. PC1 and PC2 are uncorrelated (orthogonal) over the length of the whole time series, which is a criterion of any PCA. Similar correlations and patterns of variability are maintained when either of the time series are constructed on the basis of averages of log-normalized abundances of the same species rather than the PCs (Fig. 3) (*24*). The correlation between PC2 and PC1 ($r^2 = 0.11$) over the years 1736 to 1959 is higher when PC1 is lagged by one term ($r^2 = 0.14$; 2 years) or two terms ($r^2 = 0.19$; 4 years). This lagged correlation may be a consequence of the PCA output or perhaps implies some feedback component in the physics affecting species associated with PC2 with respect to near-surface variability associated with PC1.
33. A. Bakun, *Science* **247**, 198 (1990).
34. K. M. Cobb, C. D. Charles, R. L. Edwards, H. Cheng, M. Kastner, *Nature* **424**, 271 (2003).
35. D. B. Enfield, A. M. Mestas-Nuñez, in *Inter-Hemispheric Climate Linkages*, V. Markgraf, Ed. (Academic Press, San Diego, CA, 2001), pp. 17–29.
36. The PDO is the leading principal component of SST anomalies in the North Pacific Ocean (poleward of 20°N) with the global average SST anomalies removed [(*1*); see also http://jisao.washington.edu/pdo/PDO.latest]. Thus, the PDO captures the dipole of thermal variability characterized by SST anomalies of opposite sign between the eastern Pacific and the central North Pacific, but not the SST trend. Empirical orthogonal function analysis of global SST anomalies shows that both the trend and PDO variability are strong sources of variability throughout the California Current (*35*).
37. F. Biondi, A. Gershunov, D. R. Cayan, *J. Clim.* **14**, 5 (2001).
38. R. D'Arrigo, R. Villalba, G. Wiles, *Clim. Dyn.* **18**, 219 (2001).
39. F. E. Urban, J. E. Cole, J. T. Overpeck, *Nature* **407**, 989 (2000).
40. We thank the many scientists, graduate students, technicians, and ship support at Scripps Institution of Oceanography that made this work possible. W. Berger, A. Miller, and J. C. Field provided many thoughtful discussions and comments. Supported by the Achievement Rewards for College Scientists, division Los Angeles (particularly E. and N. Carson), and S. and B. Kimmich (D.B.F.); University of California shipfunds (D.B.F.) and Coastal Initiatives grant 01T CEQI 06 1082 (D.B.F. and C.D.C.); NOAA Climate and Global Change grant NA36GP0479 and NSF Climate Dynamics grant ATM 94-06510 (T.R.B.); and NSF grants OCE96-13596 and OCE01-10300 and California Current Ecosystem LTER (M.D.O.). This is a contribution to the scientific agenda of the Eastern Pacific Consortium of the Interamerican Institute for Global Change Research.